INTERNATIONAL JOURNAL OF OPTIMIZATION IN CIVIL ENGINEERING
Int. J. Optim. Civil Eng., 2021; 11(4):611-630

EVALUATING SEISMIC RESISTANCE PARAMETERS OF OPTIMIZED REINFORCED CONCRETE MOMENT FRAMES USING AN INITIAL COST OBJECTIVE FUNCTION

M. Danesh[*, †], A. Iraji and S. Jaafari
Department of Civil Engineering, Urmia University of Technology, Urmia, Iran

ABSTRACT

The main object in optimizing reinforced concrete frames based on the performance is decreasing the initial cost or life cycle cost or total cost. The optimization performed here is with the requirement of satisfying story drifts and rotation of plastic hinges. However, this optimization may decrease seismic strength of the structure. Newton Meta-Heuristic Algorithm (NMA) was used to optimize three-, six-, and twelve-story reinforced concrete frames based on the performance and utilizing the cost objective function. The seismic parameters of the optimized frames were calculated. The results showed that the inter-story drifts at the performance level of LS controls the design. According to the results, the objective function for construction cost is not useful for the optimization of the reinforced concrete frames. Because the amounts of the over strength, the absorbed plastic energy, and the ductility factor for the optimized frames are low using the objective function for the construction cost.

Keywords: optimization; reinforced concrete frame; performance based design; newton meta-heuristic algorithm; objective function of construction cost.

Received: 18 May 2021; Accepted: 20 September 2021

1. INTRODUCTION

Cost effective design was always a challenging issue for engineers. While satisfying the design codes recommendations and limitations, engineers and researches are trying always to diminish the cost of the structures. The researchers introduced different optimization methods which diminished the construction costs. This could be attractive for the investors. Therefore, the researches were always improving and extending the optimization methods in

[*]Corresponding author: Department of Civil Engineering, Urmia University of Technology, Urmia, P.O. box 165, Iran
[†]E-mail address: m.danesh@uut.ac.ir (M. Danesh)

the recent decays. The use of the present design codes for seismic design of structures often produces overdesigned and uneconomical designs. Therefore, much attention has been paid to the issue of the optimization in the recent decays.

Optimizing reinforced concrete structures is much more complex than the optimizing steel structures. This is because of different possible dimensions for members and different possible reinforcement arrangements. For instance, arbitrary dimensions can be selected for the width and the height of the member sections during a section design. In addition, two different materials i.e. concrete and steel provide a nonhomogeneous cross-section. These issues make the optimizing of concrete structures a difficult problem [1-9]. The cross-section parameters are discrete values. On the other hand, the different complex constraints of the design codes for reinforced concrete structures make the optimization more complex [10]. The gradient based optimization methods have been used in the most of the optimization problems. The recent optimization methods for reinforced concrete structures replaced the meta-heuristic algorithms with the traditional methods.

There are two main methods for the optimization problems. The first category is gradient base and uses mathematical equations. The second category is exploratory type that optimizes the objective function directly. The evolutionary and meta-heuristic methods are categorized in the exploratory methods. These methods were developed based on the natural phenomena and the behaviors of the creatures. Among the optimization methods, the meta-heuristic algorithms are suitable for solving complex optimization problems. Each of the meta-heuristic algorithms produces random values and uses them in the optimization procedure [11]. Genetic algorithm [12], particle swarm algorithm [13], ant colony algorithm [14], eenhanced colliding bodies optimization [15], firefly algorithm [16], bat algorithm [17], finite difference algorithms [18, 19], newton algorithm [20, 21] are examples of the useful meta-heuristic algorithms.

Different researchers utilized the optimization methods to design reinforced concrete structures. Lin and Frangopol [22] optimized reinforced concrete girders using different algorithms based on the reliability. They presented the advantage of MPSO algorithm. Li et al [10] optimized reinforced concrete frames based on the force value and using the genetic algorithm. They used a set of pre-determined cross-sections with different arrangements of section dimensions and bars. Recently different methods for evaluation of the reinforced concrete structures reliability were introduced considering specific parameters with uncertainty. Fragiadakis and Papadrakakis [25] introduced an optimization method for seismic designing the reinforced concrete structures based on the reliability and the performance using the evolutionary strategy algorithm. Kaveh [26] presented many metaheuristic algorithms for design.

Some comparative studies were conducted between different optimization algorithms for designing structural frames. Kaveh and Sabzi [27] compared two optimization algorithms for reinforced concrete structures and presented the advantages of ECBO method. Gholizadeh and Aligholizadeh [28] compared four optimization methods and showed the advantages of the Algorithms. Danesh et al [20] compared the ECBO algorithm with BAT, MFA, and PSO algorithms for optimization of moment steel frames and presented the advantage of the ECBO method to others. Danesh [18] also compared FDA method to the ECBO, FA, and PSO methods and showed that the FDA method is preferable in comparison to the ECBO, FA, and PSO methods. Different researchers performed considerable works on calculation of seismic parameters of the optimized reinforced concrete and steel frames.

2. STUDIED CROSS-SECTIONS

Very different sections with different dimensions and rebar arrangements can be used for concrete beams and columns. Two databases are used for beams and columns sections. Practical limitations and constraints of ACI 318-08 were applied in producing the databases. Usually in practice, the ratio of height to width of the beams sections and columns sections are considered 1.5 through 2.5 and 1.0 through 2.0, respectively. The dimensions of the cross-sections increase with the steps of 50 mm. The bar sizes of Φ22 and Φ25 are used in the beams and the columns.

2.1 Beams

Fig. 1 shows the constraints that are applied to the beams cross-sections.

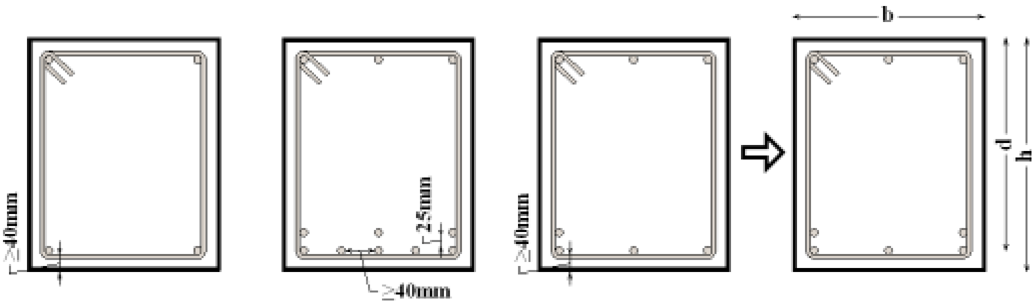

(a) (b) (c)

Figure 1. Constraints for rebar arrangement in beams

- ✓ Fig. 1a shows that at least four rebar's at the four corners of the cross-section must be considered.
- ✓ The minimum distance between longitudinal rebar's is 40.0 mm (Fig. 1b).
- ✓ The minimum concrete cover is assumed to be 40.0 mm (Fig. 1b).
- ✓ The size of the stirrup is assumed to be Φ10.
- ✓ The maximum number for rebar layers are assumed two (Fig. 1b).
- ✓ The rebar's at the top layer must be laid similar to the rebar's at the down layer. The minimum vertical distance between the two layers is 25.0 mm (Fig. 1b).
- ✓ If more rebar's are needed for a beam cross-section, they must be laid at the second top layer symmetrically with respect to the vertical axis of the cross-section. The top rebars must be laid exactly at the top of the below rebars. According to Fig. 1c, if the top rebars are not symmetrical with respect to the vertical axis, a more rebar added to satisfy the symmetry [8].

$$A_{s,min} = \frac{\sqrt{f'_c}}{4f_y} bd \ [mm^2] \qquad (1)$$

$$A_{s,max}=\frac{382.5\beta_1 f_c'}{600+f_y\, f_y}bd \ \ [mm^2] \tag{2}$$

where, b, f_c', and f_y are width of the cross-section, concrete specified compressive strength, specified yield strength of the rebars, respectively. d is effective depth of the beam and shows the distance between the centroid of the area of the tension reinforcement and the maximum compression fiber. β_1 is ratio of rectangular stress block depth to the depth of neutral axis. Rebars Φ22 are used as both of the tension and compression reinforcement [8].

Eighteen beam cross-sections are produced with applying the limitations. Dimensions of the sections were presented in Table 1.

Table 1: Beam cross-sections

No.	b (mm)	h (mm)
1	300	450
2	300	500
3	300	550
4	300	600
5	350	550
6	350	600
7	350	650
8	350	700
9	400	600
10	400	650
11	400	700
12	400	750
13	400	800
14	450	700
15	450	750
16	450	800
17	450	850
18	450	900

Totally 1014 beam cross-sections were produced. Details of some of them were presented in Table 2.

Table 2: Database used for beams [8]

No.	b (mm)	h (mm)	Number of rebars		Cost per length ($)
			Φ22 Bot.	Φ22 Top	
1	300	450	2	2	133.95
2	300	450	2	3	135.96
⋮	⋮	⋮	⋮	⋮	⋮
1013	450	900	12	10	301.78
1014	450	900	12	12	305.79

2.2 Columns

Fig. 2 illustrates constraints applied to the cross-sections of the columns according to ACI 318-08. The details of the constraints are as follows:

- ✓ a. The minimum free distance between the longitudinal rebars must be 40.0 mm (Fig. 2b).
- ✓ b. At least four rebars must be laid at the four corners of the cross-section (Fig. 2b).
- ✓ c. The minimum of the concrete cover assumed to be 40.0 mm (Fig. 2b).
- ✓ d. The stirrup size assumed to be Φ10.
- ✓ e. The rebars must be symmetrical with respect to the vertical and horizontal axes (Fig 2b).
- ✓ f. The minimum and maximum longitudinal reinforcement ratio are limited to 1% and 8%, respectively.

The rebars used for the columns are Φ25.

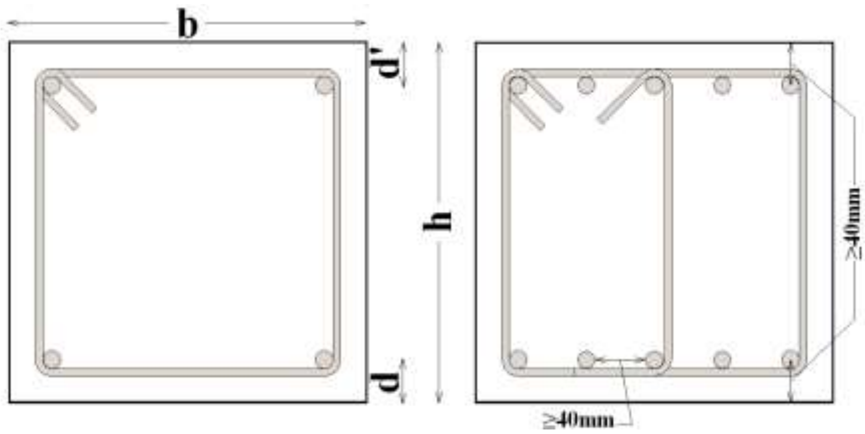

(A) (B)

Figure 2. Constraints for columns cros-sections

The strength of each column under flexural and axial loads were calculated using P-M interaction diagrams. Fig. 3 illustrates a linear simplified P-M interaction diagram used in this paper [8].

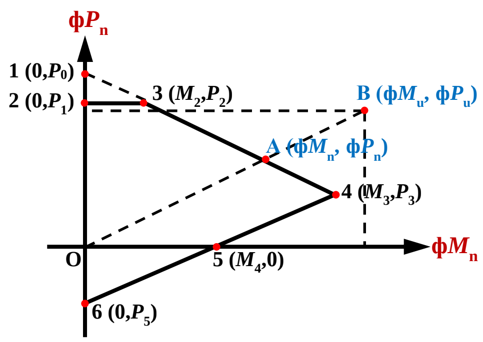

Figure 3. Linear P-M interaction diagram using specified points [8]

OA and OB are calculated as follows:

$$L_{OA} = \sqrt{(\emptyset M_n)^2 + (\emptyset P_n)^2} \qquad L_{OB} = \sqrt{(M_u)^2 + (P_u)^2} \tag{3}$$

If the inequality $L_{OB} \leq L_{OA}$ is satisfied, the column design will be safe.

Table 3 shows the database for the cross-sections of the columns used in this research. The number of columns cross-sections in the database is 55. The range for the dimensions of the cross-sections is 300.0 mm ~ 900.0 mm with increasing steps of 50.0 mm. The method of the cost calculation will be described in the next sub-sections.

Table 3: Database used for columns cross-sections [8]

No.	b (mm)	h (mm)	Number of rebars Φ25	Cost per length ($)
1	300	300	4	133.72
2	300	300	6	140.66
⋮	⋮	⋮	⋮	⋮
54	900	900	22	492.55
55	900	900	24	499.48

3. METHOD OF ANALYSIS AND DESIGN

To optimize the structure design, all of the design constraints must be satisfied. Internal forces including the bending moments, the axial forces, and the shear forces are required to check the constraints. The internal forces can be determined using finite element method. To simplify the procedure, only the bending moments of the beams were applied in the calculations. Both of the axial forces and the bending moments were applied in the columns optimization. The analysis method checks the slenderness of the columns and if a column is slender the slenderness factor will be applied to the column design.

When a column is slender the moment magnification procedure should be considered. Slenderness effect can be neglected for columns not braced against sidesway when:

$$\frac{kl_u}{r} < 22 \tag{4}$$

where, k effective length factor, l_u unbraced column length and r radius of gyration for compression member. The effective length factor k is calculated using the stiffness ratio ψ at the ends of the column. This ratio is calculated by dividing the sum of the stiffnesses of the columns at a joint by the sum of the stiffnesses of the flexural members framing into that joint in the analysis direction:

$$\psi=\frac{\Sigma\left(\frac{EI}{l}\right)_{c}}{\Sigma\left(\frac{EI}{l}\right)_{b}} \tag{5}$$

where, I inertia moment of cracked section, E modulus of elasticity; l center-to-center length of a beam or a column. Indices b and c indicates beam and column, respectively. ψ is calculated for two ends of the column and then the average of ψ i.e. ψ_m is calculated. The effective length factor is calculated as follows:

$$\psi_{m}<2 : k=\left(1\text{-}0.05\psi_{m}\right)\sqrt{1+\psi_{m}} \tag{6}$$

$$\psi_{m}\geq 2 : k=0.9\sqrt{1+\psi_{m}} \tag{7}$$

The magnified moment for a slender column is calculated as follows:

$$M=M_{ns}+\delta_{s}M_{s} \tag{8}$$

M_{ns} is the factored moment due to loads that cause no appreciable sidesway and M_s is the factored moment that due to loads that cause appreciable sidesway. δ_s is moment-magnification factor for unbraced frames against lateral displacements. The magnified moment is calculated for two ends of the column and then the maximum of those is selected for column design.

The specified compressive strength of the concrete and the specified yield strength of the rebars are assumed 24.0 MPa and 352.0 MPa, respectively. The analysis and design of the frames are performed using MATLAB [36] and OpenSees [37] by connecting of them to each other.

4. FORMULATION FOR OPTIMIZATION

The construction cost consists of concrete placing, the reinforcement, and form-working. Objective functions of these three parts are formulated as follows:

$$C=C_{Column}+C_{Beam} \tag{9}$$

$$C_{Column}=\sum_{i=1}^{nc}\left[b_{c.i}h_{c.i}C_{C}+A_{S.c.i}C_{S}+2\left(b_{c.i}+h_{c.i}\right)C_{F}\right]H_{i} \tag{10}$$

$$C_{Beam}=\sum_{j=1}^{nb}\left[b_{b.j}h_{b.j}C_{C}+A_{S.b.j}C_{S}+\left(b_{b.j}+2h_{b.j}\right)C_{F}\right]L_{j} \tag{11}$$

where, C_{Column} and C_{Beam} are costs of columns and beams, repectively. nc and nb are numbers of columns and beams, respectively. $b_{c.i}$, $h_{c.i}$, H_i and $A_{S.c.i}$ are width, depth, height, and reinforcement area for ith column cross-section, respectively. $b_{b.j}$, $h_{b.j}$, L_j, and $A_{S.b.j}$ are width, depth, length, and reinforcement area for jth beam cross-section, respectively. C_C, C_S, and C_F are the cost per cubic meter for concrete, the cost per cubic meter for reinforcement, and the cost for squared meter for form-working, respectively, as follows [1-9]:

$$\mathrm{C_C}=105\,\frac{\$}{\mathrm{m}^3}\ ,\ \mathrm{C_S}=7065\,\frac{\$}{\mathrm{m}^3}\ ,\ \mathrm{C_F}=92\,\frac{\$}{\mathrm{m}^2}$$

The frames were analyzed for load combinations as follows:

$$1.2D+1.6L \tag{12}$$

$$1.2D+1.0L\pm1.0E \tag{13}$$

$$0.9D\pm1.0E \tag{14}$$

The maximum internal forces from the load combinations are determined. D and L are dead and live loads that were assumed 32.6 kN/m2 and 13 kN/m2, respectively. The number of rebars and cross-section dimensions of the columns (n_T,b_T) in the top stories must not be greater than those (n_B,b_B) of the bottom story. The width of the beams at the joints must not be greater than that of the columns at the same joints. The practical and design constraints for the frames are as follows:

$$g_1=\frac{\mathrm{M_u^+}}{\emptyset\mathrm{M_n^+}}-1\leq 0 \tag{15}$$

$$g_2=\frac{|\mathrm{M_{uL}^-}|}{\emptyset\mathrm{M_n^-}}-1\leq 0 \tag{16}$$

$$g_3=\frac{|\mathrm{M_{uR}^-}|}{\emptyset\mathrm{M_n^-}}-1\leq 0 \tag{17}$$

$$g_4=\frac{L_{OB}}{L_{OA}}-1\leq 0 \tag{18}$$

$$g_5=\frac{b_T}{b_B}-1\leq 0 \tag{19}$$

$$g_6=\frac{h_T}{h_B}-1\leq 0 \tag{20}$$

$$g_7=\frac{n_T}{n_B}-1\leq 0 \tag{21}$$

After checking the constraints, a gravity load combination according to ASCE41-13 [38] is subjected to the frames as follows:

$$Q_u^{PBD}=D+0.25L \tag{22}$$

Normalized shape modes are subjected to the frames and then the push-over analysis is performed. The frames are checked for the performance constraints such as the drift, the rotations of plastic hinges and the strong column-weak beam concept as follows:

$$g_8 = \frac{D_j^i}{D_{all}^i} - 1 \leq 0 \quad j=1,2,....ns \tag{23}$$

$$g_9 = \frac{\theta_j^i}{\theta_{all}^i} - 1 \leq 0 \quad j=1,2,....nc \tag{24}$$

$$g_{10} = \frac{\theta_k^i}{\theta_{all}^i} - 1 \leq 0 \quad k=1,2,....nb \tag{25}$$

where, D_j^i and D_{all}^i $i=IO;LS;CP$ are the drift of jth story and allowable drift for the concrete moment frame according to FEMA-35, respectively [39]. The allowable drifts for the three performance levels of IO, LS, and CP are limited to 1%, 2%, and 4%, respectively. *ns* is number of stories, θ_j^i and θ_k^i are the maximum rotation of the plastic hinge for the columns and the beams, respectively. θ_{all}^i is the allowable value for the rotation of the plastic hinge for the beams and the columns according to ASCE 41-13 [38]. *nc* and *nb* are the total number of the columns and the beams, respectively.

The column failure is more dangerous than the beam failure during an earthquake. ACI 318-08 introduces the concept of the strong column-weak beam as a basic principle to design special moment-resisting frames. This code indicates that the plastic hinge in the columns must occur later than the beams. This behavior prevents the structure collapse during strong earthquakes. The sum of nominal moment strengths of the columns must be greater than 1.2 times the sum of the nominal moment strengths of the beams at a joint according to ACI 318-08:

$$g_{11} = \frac{1.2 \times (\mathrm{M}_{\mathrm{nb}}^{+} + \mathrm{M}_{\mathrm{nb}}^{-})}{(\mathrm{M}_{\mathrm{nc}}^{\mathrm{top}} + \mathrm{M}_{\mathrm{nc}}^{\mathrm{bot}})} - 1 \leq 0 \tag{26}$$

where, $\mathrm{M}_{\mathrm{nb}}^{+}$ and $\mathrm{M}_{\mathrm{nb}}^{-}$ are nominal bending moments of the beams at two sides of the joints. $\mathrm{M}_{\mathrm{nc}}^{\mathrm{top}}$ and $\mathrm{M}_{\mathrm{nc}}^{\mathrm{bot}}$ are nominal bending moments of the columns at the top and the bottom of the joint, respectively. The optimization constraints are applied in the objective function using exterior penalty function method (EPFM) [40]. The objective function is formulated as follows:

$$\Phi = C \times r_p \times (1 + P_{El} + P_{Dr} + P_{Rot} + P_{SCWB}) \tag{27}$$

where, P_{El}, P_{Dr}, P_{Rot}, and P_{SCWB} are penalty functions for the practical and design constraints, the drift, the rotation of the plastic hinge, and the strong column-weak beam, respectively. r_p is the penalty coefficient. These penalty functions are defined as follows:

$$P_{El}=\sum_{i=1}^{nb}\sum_{j=1}^{3}\left(\left(\max\left\{0,g_j\right\}\right)^2\right)_i+\sum_{i=1}^{nc}\sum_{j=4}^{7}\left(\left(\max\left\{0,g_j\right\}\right)^2\right)_i \quad (28)$$

$$P_{Dr}=\sum_{i=1}^{ns}\sum_{j=1}^{3}\left(\left(\max\left\{0,g_8\right\}\right)^2\right)_i \quad (29)$$

$$P_{Rot}=\sum_{i=1}^{ns}\sum_{j=1}^{3}\left(\left(\max\left\{0,g_{j+8}\right\}\right)^2\right)_i+\sum_{i=1}^{ns}\sum_{j=1}^{3}\left(\left(\max\left\{0,g_{j+9}\right\}\right)^2\right)_i \quad (30)$$

$$P_{SCWB}=r_p\sum_{i=1}^{nj}\left(\max\left\{0,g_{11}\right\}\right)^2 \quad (31)$$

5. NUMERICAL EXAMPLES

5.1 Three-story frame

Fig. 4 illustrates the three-story frame geometry, lateral loads, and the types of the columns and the beams.

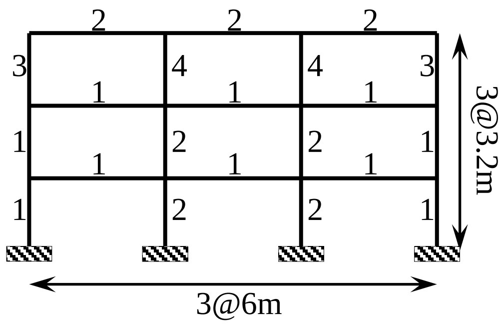

Figure 4. Three-story concrete frame

Table 4 shows the optimized results from the Newton Meta-Heuristic Algorithm. Fig. 5 shows the profiles for the drifts of the stories at the performance levels of IO, LS, and CP. According to the results, the constraint for the drift at the performance level of LS controls the design. The Demand-Capacity ratio for the rotation of the plastic hinges is presented in Fig. 6. The beams and the columns were separated via a red line in this Figure.

Table 4: Optimized design for three-story frame

Element		Dimensions		Rebars		Total cost ($)	Number of analyses
Type	Group	b (mm)	h (mm)	Bot.	Top		
Beam	1	400	500	2Φ22	5Φ22	16313	5000
	2	400	400	2Φ22	6Φ22		
Column	1	400	400	6Φ25			
	2	450	450	10Φ25			
	3	400	400	6Φ25			
	4	400	400	6Φ25			

5.2 Six-story frame

Fig. 7 shows the geometry, the lateral loads, and the types of the beams and the columns for the six-story frame. Six types for the columns and three types for the beams were used in the optimization. Table 5 shows the optimized design using the Newton Meta-Heuristic Algorithm. Fig. 8 illustrates the profiles for inter-story drifts at the performance levels of IO, LS, and CP. Fig. 9 shows the demand-capacity ratio of the plastic hinge rotation for the columns and the beams. According to the results, the drift constraints at the performance level of LS controls the design.

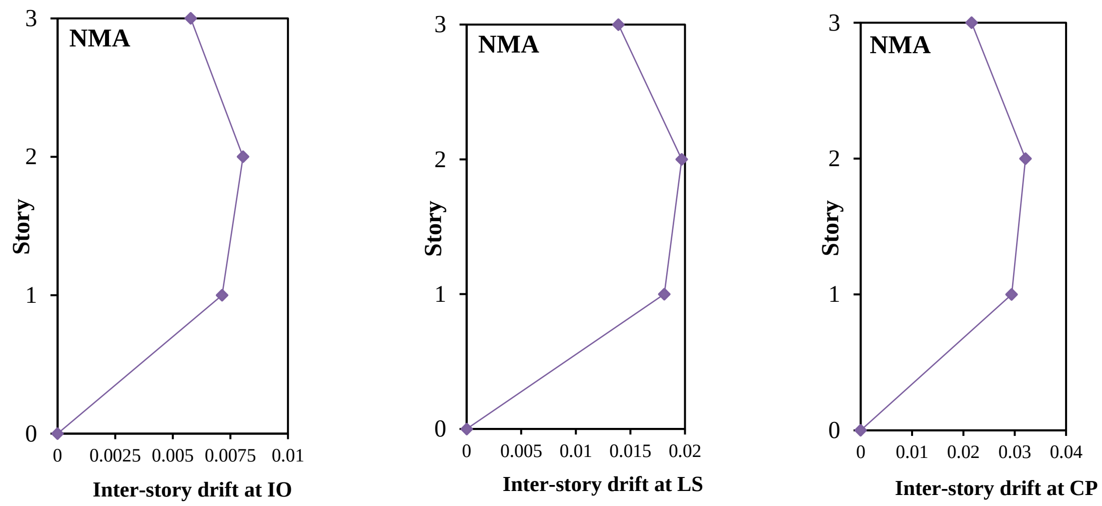

Figure 5. Profiles of inter-story drifts for three-story frame at performance levels of IO, LS, and CP

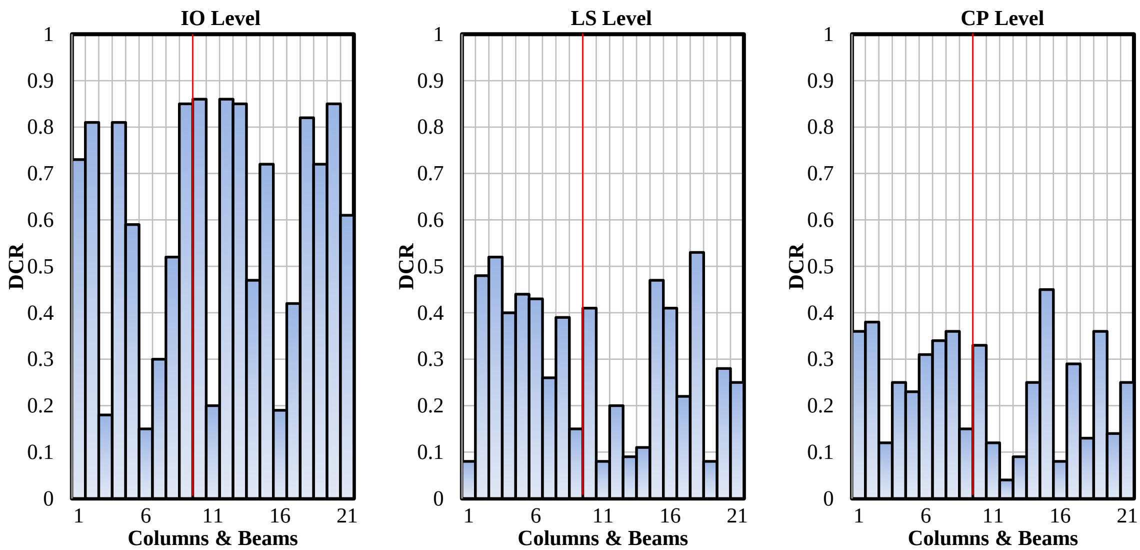

Figure 6. Bar charts of demand-capacity ratio of plastic hinge rotation for columns and beams at performance levels of IO, LS, and CP, three-story frame

5.3 Twelve-story frame

Fig. 10 illustrates the geometry, the lateral loads, and the types of the columns and the beams for the twelve-story frame. Nine and five types applied in the optimization for the columns and the beams, respectively. Table 6 shows the optimizaed design using the Newton Meta-Heuristic Algorithm. Fig. 11 shows the profiles of the inter-story drifts at the performance levels of IO, LS, and CP. Fig. 12 shows the demand-capacity ratio of the plastic hinge rotation for the beams and the columns. The results show that the drift constraints at the performance level of LS controls the design.

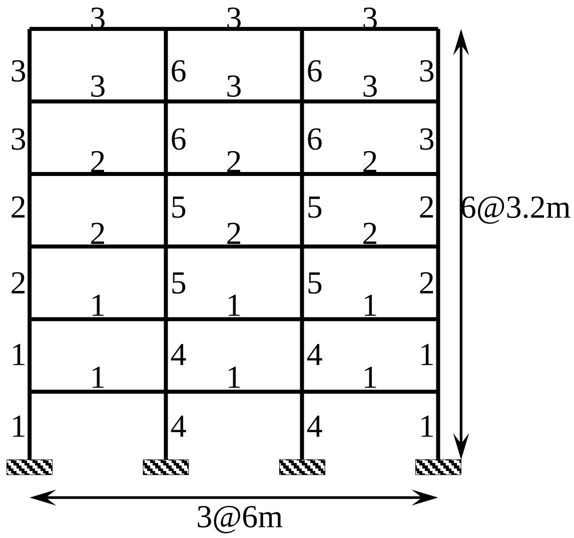

Figure 7. Six-story concrete frame

Table 5: Optimized design for six-story frame

Element		Dimensions		Rebars		Total cost ($)	Number of analyses
Type	Group	b (mm)	h (mm)	Bot.	Top		
Beam	1	350	650	2Φ22	3Φ22	39120	17000
	2	350	550	2Φ22	6Φ22		
	3	350	550	2Φ22	4Φ22		
Column	1	550	550	8Φ25			
	2	550	550	8Φ25			
	3	400	400	6Φ25			
	4	650	650	12Φ25			
	5	550	550	12Φ25			
	6	450	450	8Φ25			

6. EVALUATION OF SEISMIC PARAMETERS OF OPTIMIZATION

The optimizaed frames are analyzed via nonlinear static method according to the FEMA-356. The produced capacity diagrams are converted to bi-linear diagrams using Yang method. Then, the seismic strength parameters are extracted from the results.

6.1 Three-story frame

Fig. 13 shows the bi-linear capacity diagram for the three-story frame. Table 7 shows the seismic strength parameters for the three-story frame. The results show low amounts for the over strength and the absorbed plastic energy for the three-story frame. This can be attributed to the optimization of this frame using the objective function for the construction cost. Because the structure satisfies the design constraints, the service, and the performance using the minimum materials, therefore it cannot experience high over strength and ductility at the state of nonlinear – inelastic behavior.

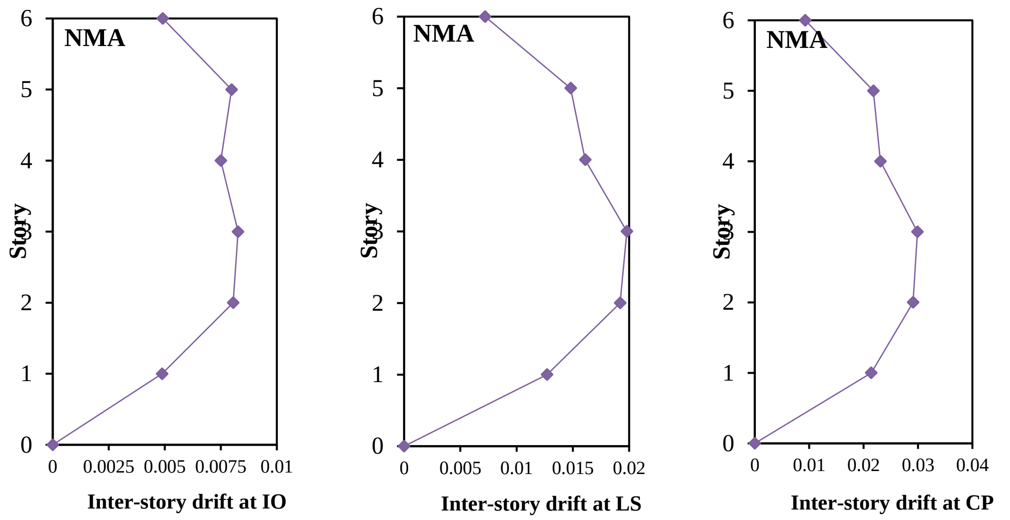

Figure 8. Profiles of inter-story drifts for six-story frame at performance levels of IO, LS, and CP

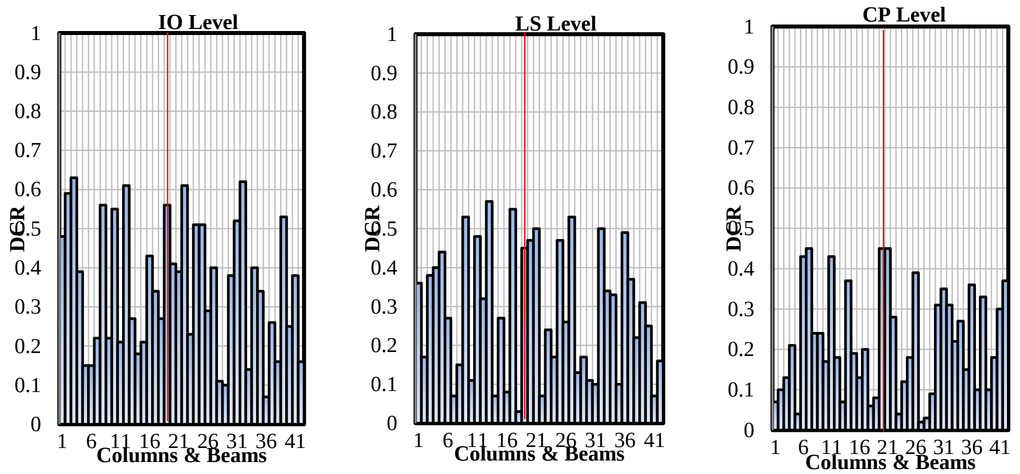

Figure 9. Bar charts of demand – capacity of plastic hinge rotation for columns and beams at performance levels of IO, LS, and CP, six story frame

6.2 Six-story frame

Fig. 14 shows the bi-linear diagram for the capacity of the six-story frame. Table 8 shows the seismic strength parametrs of the optimized six-story frame. Because the frame was optimized using the objective function for the construtction cost, the over strength and the amount of the absorbed energy for the frame are very low. The optimization provides the minimum materials for the design while satisfies the design constraints and the needed service and performance. Applying the minimum materials, the structure cannot provide high over strength and ductility at the state of nonlinear – inelastic behavior.

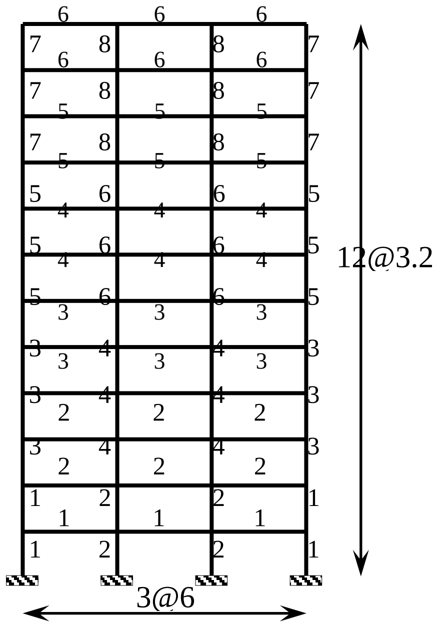

Figure 10. Twelve-story concrete frame

Table 5: Optimized design of twelve-story frame

Element		Dimensions		Rebars		Total cost ($)	Number of analyses
Type	Group	b (mm)	h (mm)	Bot.	Top		
Beam	1	800	550	4Φ22	7Φ22	101524	60000
	2	700	550	4Φ22	6Φ22		
	3	600	550	3Φ22	6Φ22		
	4	550	550	3Φ22	5Φ22		
	5	500	550	3Φ22	4Φ22		
	6	450	550	3Φ22	3Φ22		
Column	1	800	800	24Φ25			
	2	800	800	24Φ25			
	3	800	800	20Φ25			
	4	700	700	20Φ25			
	5	700	700	20Φ25			
	6	600	600	16Φ25			
	7	550	550	12Φ25			
	8	500	500	8Φ25			

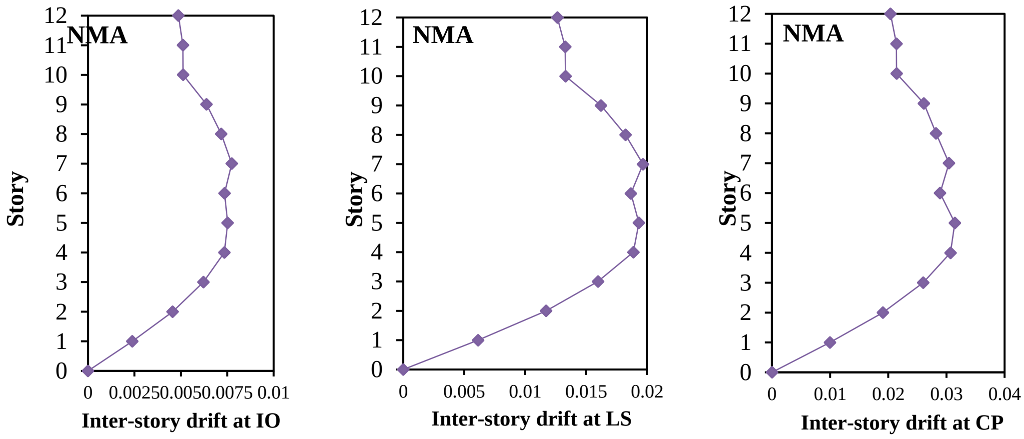

Figure 11. Profiles of inter-story drifts for twelve-story frame at performance levels of IO, LS, and CP

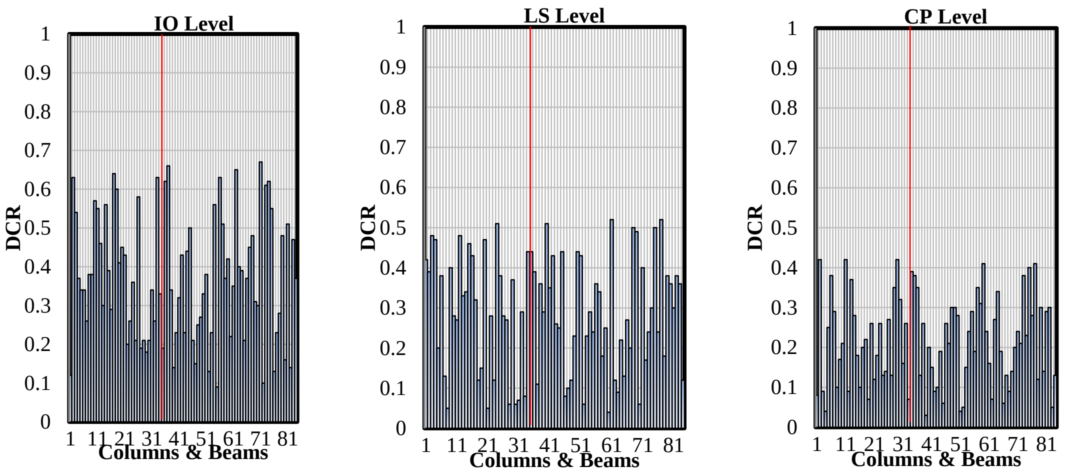

Figure 12. Bar charts of demand – capacity of plastic hinge rotation for columns and beams at performance levels of IO, LS, and CP, twelve-story frame

Table 7: Seismic strength parameters of optimized three-story frame

Parameter	over strength	Plastic displacement (mm)	Ductility factor	Initial stiffness	Final stiffness	Absorbed energy (kN.m)	Behavior factor	Fundamental period (s)
Value	0.47	236.74	9.57	11894.59	319.42	152585	7.32	0.575

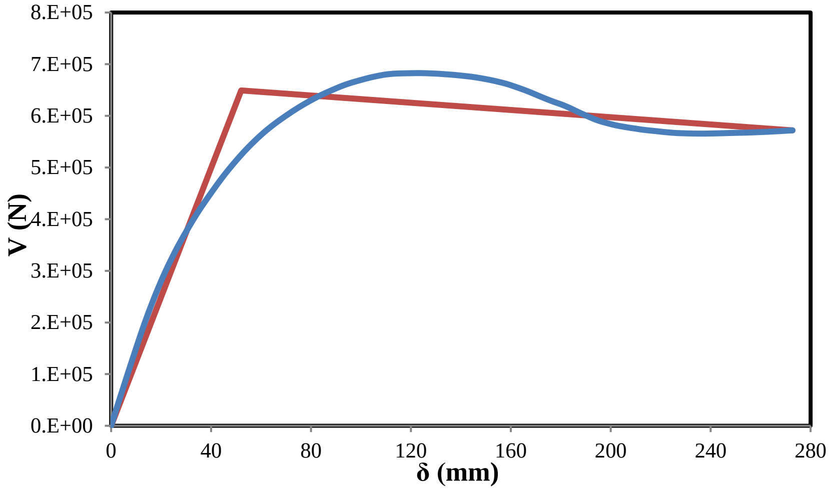

Figure 13. Bi-linear diagram of capacity for three-story frame using Yang method

Table 8. Seismic strength parameters of optimized six-story frame

Parameter	over strength	Plastic displacement (mm)	Ductility factor	Initial stiffness	Final stiffness	Absorbed energy (kN.m)	Behavior factor	Fundamental period (s)
Value	0.15	314.72	6.31	16050.64	971.90	264443	7.84	1.000

6.3 Twelve-story frame

Fig. 15 illustrates the bi-linear diagram of the capacity for the twelve-story frame. Table 9 shows the seismic strength parametrs of the twelve-story frame. The results show low amounts for the over strength and the absorbed plastic energy. This is attributed to optimizing this frame using the objective fuction for the construction cost. Because the optimization gives minimum amount for materials and satisfies the design constraints, the needed service and performance, therefore, the structure cannot provide the high over strength and ductility during the nonlinear – inelastic behavior.

Table 9. Seismic strength parameters of optimized twelve-story frame

Parameter	over strength	Plastic displacement (mm)	Ductility factor	Initial stiffness	Final stiffness	Absorbed energy (kN.m)	Behavior factor	Fundamental period (s)
Value	0.09	547.63	8.16	19623.21	1105.27	2724590	7.61	1.970

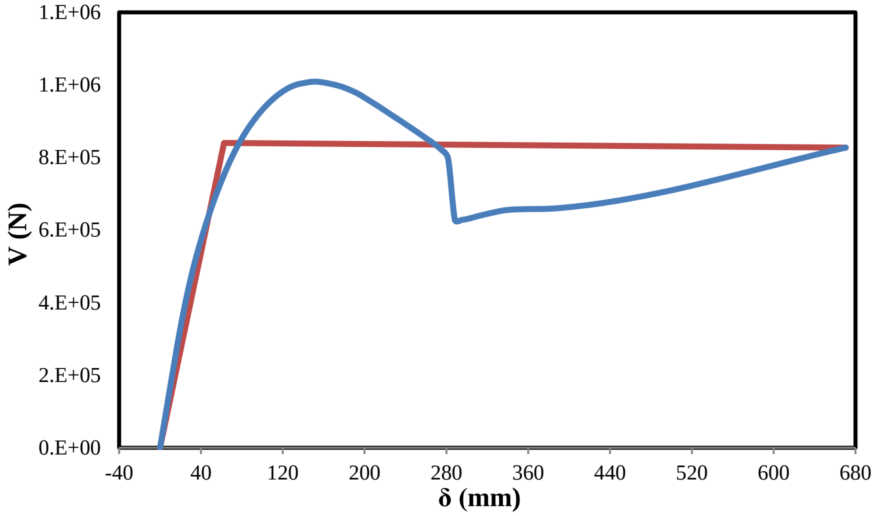

Figure 14. Bi-linear diagram of capacity for six-story frame using Yang method

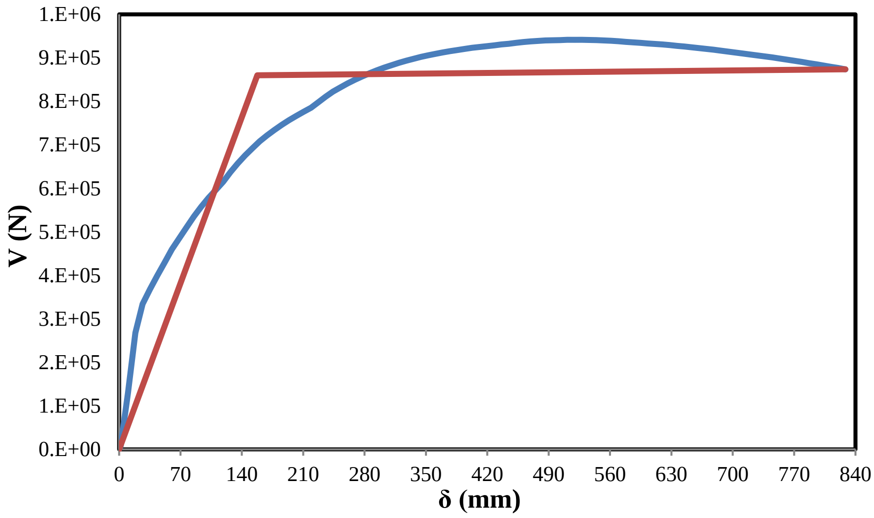

Figure 15. Bi-linear diagram of capacity for twelve-story frame using Yang method

7. CONCLUSIONS

Three-story, six-story, and twelve-story frames were optimized using Newton Meta-Heuristic Algorithm using the objective function for the construction cost and design, service, strength, and performance constraints. The optimized frames were analyzed using the nonlinear static method. The bi-linear diagram for the capacity was provided using the Yang method. Then, the seismic strength parameters were extracted.

The optimization procedure showed that the constraint of inter-story drifts has a decisive role. With satisfying this constraint, other constraints such as the plastic hinge rotation and the strong column – weak beam concept are satisfied simply.

The low amounts for the over strength, the absorbed plastic energy, and the ductility factor for the optimized frames using the objective function of the initial cost shows that this function is not suitable for the seismic optimization based on the performance of the reinforced concrete frames. Therefore, the objective function of the total cost is prefarable to the objective function of the initial cost. The total cost consisits of the construction and service costs. If the use of the only initial cost is unavoidable, the choice of the values for the performance costraints must be more strict than the constraints of the design codes.

REFERENCES

1. Zou XK. Optimal seismic performance-based design of reinforced concrete buildings, *Structural Seismic Design Optimization and Earthquake Engineering: Formulations and Applications* 2012; IGI Global; pp. 208-231.
2. Fragiadakis M, Papadrakakis M. Performance-based optimum seismic design of reinforced concrete structures, *Earthq Eng Struct Dyn* 2008; **37**(6): 825-44.
3. Khatibinia M, Gharehbaghi S, Moustafa A. Seismic reliability-based design optimization of reinforced concrete structures including soil-structure interaction effects, *Earthquake Engineering-From Engineering Seismology to Optimal Seismic Design of Engineering Structures* 2015; InTech.
4. Khatibinia M., et al. Reliability-based design optimization of reinforced concrete structures including soil–structure interaction using a discrete gravitational search algorithm and a proposed metamodel, *Eng Optim* 2013; **45**(10): 1147-65.
5. Park RL, Park R, Paulay T. *Reinforced Concrete Structures*, John Wiley & Sons, 1975.
6. Gholizadeh S, Aligholizadeh V. Optimum design of reinforced concrete frames using bat meta-heuristic algorithm, *Eng Optim* 2013; **45**(11): 254-72.
7. Zou XK, Chan CM. Optimal seismic performance-based design of reinforced concrete buildings using nonlinear pushover analysis, *Eng Struct* 2005; **27**(8): 1289-1302.
8. Kaveh A, Sabzi O. A comparative study of two meta-heuristic algorithms for optimum design of reinforced concrete frames, *Int J Civil Eng* 2011; **9**(3): 193-206.
9. Haselton CB, et al. An assessment to benchmark the seismic performance of a code-conforming reinforced-concrete moment-frame building, *Pacific Earthq Eng Res Center* 2008: (2007/1).
10. Lee C, Ahn J. Flexural design of reinforced concrete frames by genetic algorithm, *J Struct Eng* 2003; **129**(6): 762-74.
11. Gholizadeh S, Sojoudizadeh R. modified sine-cosine algorithm for sizing optimization of truss structures with discrete design variables, *Int J Optim Civil Eng* 2019; **9**(2): 195-212.
12. Rajeev S, Krishnamoorthy C. Discrete optimization of structures using genetic algorithms, *J Struct Eng* 1992; **118**(5): 1233-50.
13. Kennedy J, Eberhart RC. A discrete binary version of the particle swarm algorithm, *Systems, Man, and Cybernetics* 1997, *IEEE International Conference*.
14. Kaveh A, Farahmand Azar, B, Hadidi, A, et al. Performance-based seismic design of steel frames using ant colony optimization, *J Construct Steel Res* 2010; **66**(4): 566-74.

15. Kaveh A, Ilchi Ghazaan M. Enhanced whale optimization algorithm for sizing optimization of skeletal structures, *Mech Based Des Struct Mach* 2017; **45**(3): 345-62.
16. Yang XS. Firefly algorithms for multimodal optimization, *Int Sympos Stoch Algorith* 2009; **44**: 181-91.
17. Yang XS. A new metaheuristic bat-inspired algorithm, *Nature Inspir Cooperat Strateg Optim* 2010; **55**: 65-74.
18. Danesh M. Evaluation of seismic performance of PBD optimized steel moment frames by means of neural network, *Jordan J Civil Eng* 2019; **13**(3): 43-68.
19. Danesh M, Iraji A. Performance-based layout optimization for braced steel frames using finite difference algorithm, *Int J Optim Civil Eng* 2020; **10(4)**: 651-68.
20. Danesh M, Gholizadeh S, Gheyratmand C. Performance-based optimization and seismic collapse safety assessment of steel moment frames, *Int J Optim Civil Eng* 2019; **9**(3): 483-98.
21. Danesh M, Jalilkhani M. Sizing optimization of truss structures with Newton meta-heuristic algorithm, *Int J Optim Civil Eng* 2020; **10**(3): 433-50.
22. Lin KY, Frangopol DM. Reliability-based optimum design of reinforced concrete girders. *Struct Safe* 1996; **18**(2-3): 239-58.
23. Möller O. et al. Structural optimization for performance-based design in earthquake engineering: Applications of neural networks, *Struct Safe* 2009; **31**(6): 490-9.
24. Möller O. et al. Seismic structural reliability using different nonlinear dynamic response surface approximations, *Struct Safe* 2009; **31**(5): 432-42.
25. Fragiadakis M, Papadrakakis M. Performance-based optimum seismic design of reinforced concrete structures, *Earthq Eng Struct Dyn* 2008; **37**(6): 825-44.
26. Kaveh A. Advances in metaheuristic algorithms for optimal design of structures, 3rd edition, Springer, 2021.
27. Kaveh A, Sabzi O. A comparative study of two meta-heuristic algorithms for optimum design of reinforced concrete frames, *Eng Optim* 2011; **44**(7): 115-31.
28. Gholizadeh S, Aligholizadeh V. Optimum design of reinforced concrete frames using bat meta-heuristic algorithm, *Int J Optim Civil Eng* 2013; **3**(3): 483-97.
29. Alam Z, Zhang C, Samali B. The role of viscoelastic damping on retrofitting seismic performance of asymmetric reinforced concrete structures, *Earthq Eng Eng Vib* 2020; **19**(1): 223-37.
30. Di Trapani, F. et al. Optimal seismic retrofitting of reinforced concrete buildings by steel-jacketing using a genetic algorithm-based framework, *Eng Struct* 2020; **219**: 110864.
31. Martins AM, Simões LM, Negrão JH. Optimization of extradosed concrete bridges subjected to seismic action, *Comput Struct* 2021; **245**: 106460.
32. Jiang L. et al. Seismic life-cycle cost assessment of steel frames equipped with steel panel walls, *Eng Struct* 2020; **211**: 110399.
33. Montuori R. et al. A simplified performance based approach for the evaluation of seismic performances of steel frames, *Eng Struct* 2020; **224**: 111222.
34. Degertekin S, Tutar H, Lamberti L. School-based optimization for performance-based optimum seismic design of steel frames, *Eng Comput* 2020; **214**: 1-15.
35. Committee A, Institute AC, I.O.f. Standardization. Building code requirements for structural concrete (ACI 318-08) and commentary 2008, American Concrete Institute.

36. MathWorks, MATLAB: the language of technical computing. Desktop tools and development environment, version **7**. Vol. **9**. 2005: MathWorks.
37. Gu Q, Conte J, Barbato M. OpenSees command language manual response sensitivity analysis based on the direct differentiation method (DDM), Berkeley, CA: Pacific Earthquake Engineering Center, University of California 2010.
38. Committee A.S.S.R.S. Seismic rehabilitation of existing buildings (ASCE/SEI 41-06). American Society of Civil Engineers, Reston, VA 2007.
39. Council B.S.S. Prestandard and commentary for the seismic rehabilitation of buildings. Report FEMA-356, Washington DC 2000.
40. Vanderplaats GN. Numerical optimization techniques for engineering design, Vanderplaats Research and Development, Incorporated, 2001.